XIV. Congress of the International Society of Photogrammetry
Hamburg 1980
Commission III
Working Group WG III-1
Presented Paper
Walter Schuhr
Institute for Photogrammetry and Eng. Surv.
University Hannover, West Germany

ANALYSIS AND APPLICATION OF ALGORITHMSFOR DIGITAL ORTHOPHOTOS

Abstract: The purpose for digital geometric image processing is to provide digital orthophotos for the benefit of classification, texture analysis, change detection or in view of a map alternative. This investigation especially deals with modular multispectral scanner data (M^2S, Bendix) and Landsatdata. Instead of manual counting in the lineprinterimage, imagecoordinates were gathered by PSK comparator measurements. For detecting gross errors second order polynomial approaches have been successfully applied. Owing to the availability of simultaneous conventional aerial photography, map coordinates and exterior orientation data were gained from conventional bundle block adjustment. A development of this inflight data using fifth order polynomials resulted into a position accuracy for x_0', y_0' and z_0' of about $\pm$ 10 m. Subsequently a bundle block adjustment approach for scanner-imagery including additional parameters (distortion terms in x' and y') in the collinearity equations was applied, as far as overlapping imagery is concerned. In the case of single pictures, resection in space was used, where also the flow in of the (calculated) exterior orientation data can be chosen. The mean square adjustment procedure is based on numerial differentiation. Compensation of errors initiated from the rough mathematical model and from the application of the analysed dynamic data by interpolation using the weightened mean method resulted into an accuracy of about $\pm$ 1.4 pixels, using 41 independent checkpoints (126 ground controlpoints).

In the next chapter the data analysis is followed by the pixelwise rectification, using the inverse method. Here DTM data is calculated by hyperbolic interpolation. With respect to program optimizing, the anchropoint - and the nearest neighbourhood method for the grey value interpolation are applied. The computertime for a CDC Cyber 76 - 12 large computer is about 1 minute for 1000 x 1000 pixels, equivalent to 63 µs/pixel. The Fortran and Compass programs have been developed under Prof. Konecny at the Institute for Photogrammetry and Eng. surv. of the University of Hannover and at the Sonderforschungsbereich 149 S1 in coordination with the DFVLR/Oberpfaffenhofen.

1. Elementaries:

This investigation requires three different types of data independent of the used rectification method:

1.1 Computer Compatible Tapes (C.C.T.s) with stored scannerdata (greyvalues) on a magnetic disc. After a histogram linearization the grey values are copied on a line printer or on an Optronics P 1700 device.

1.2 The D.T.M. data, gained from maps or from photogrammetric model evaluation, following Rüdenauer /1/, are stored on another magnetic disc.

1.3 The ground control point coordinates, can for instance be gathered from big scale topographic maps (TK 25 or DGK 5) or result from conventional aerial photography bundle block adjustment. As simultaneous aerial photography was available, map coordinates were derived from conventional bundle block adjustment within an accuracy of ± 2.0 m, following Jacobsen /2/. In the case of simultaneous conventional aerial photography and M^2S imagery the usual fiducial marks, which are only visible in conventional photographs are sufficient. The geometric connection with the scanner images then happens by means of not signaled but sharp contoured points, which can be interpreted in the images of both sensors. By this means errors in pointidentification due to deficient map updating largely have been avoid. The image coordinates of the ground control points, as there are centers of highway-, road- or way-crossings, bridges, small sees, small islands, tree shadows etc. succeeded within an interior accuracy of ± 10 µm from Zeiss PSK comparator measurements in the unrectified halftone image, followed by an affine transformation based on the four image edges for which ± 0.1 pixel have been reached. Besides this, rows and column values can be gathered from manual counting in a lineprinter image or on an interactive screen (for instance MDAS/Bendix, DIBIAS/DFVLR), if the zoom effect is implemented.

Data experiments are devided into two main projects, following Baker /3/, Anuta /4/ and Bernstein /5/:

1. The solution of the orientation parameters, which are valid for the image or for the whole block, by computing image coordinates from ground control point coordinates and maybe from in flight data.
2. In a second step the actual digital rectification is practizised by applying this orientation parameters onto the pixels.

Results from a staying in the States in 1976, where the author accompanied Prof. Konecny and Prof. Wrobel, showed, there is only the Purdue university, where collinearity equations are used as a rectification algorithm, in which we also believe in Hannover, as many other institutes use rubber sheet stretch approaches.
In principle correction parameters can result from image correlation but only, if the correlation can be based on any second image, which is not a condition of this subject.

2. Direct or inverse method?

The direct rectification method uses image coordinates of the unrectified (two dimensional) image to calculate the map positions ($x_i y_i$) for the grey values, under the condition of known z_i. On the other hand the indirect method computes for every three dimensional output pixel position the image position and hence the row - and column position for the grey value. Obviously the direct method only allows an iterative calculation of the terrain hights (D.T.M.).
Looking onto the obtainable accuracy both methods are equivalent. The methods are sensitive for positions of evolution:

1. In fact of pixel by pixel rectification for the direct method the computed DTM positions are interpreted as if they are measured.

2. For the indirect method the exterior orientation parameters for the output pixels (x, y, z) can not expressed as a function of the measured image coordinates, after which the orientation parameters have been developed in the checkpoint analysis.
One big advantage of the indirect method is the easy generating of rectilinear limited data blocks, which is not that simple to get using the direct method. Looking onto the practical qualification the indirect method should be prefered.

3. Dataanalysis

The following analysis serves for the purpose to determin parameters in a mathematical model which proper fits to the physical reality and is valid for the whole scenery. According to Konecny /6/ the collinearity equations for scanner imagery are

$$\Delta x' = -c\,\frac{a_{11j}(x_i - x'_{oj}) + a_{12j}(y_i - y'_{oj}) + a_{13j}(z_i - z'_{oj})}{a_{31j}(x_i - x'_{oj}) + a_{32j}(y_i - y'_{oj}) + a_{33j}(z_i - z'_{oj})}$$

and (1)

$$c \cdot \tan\theta_{ij} = -c\,\frac{a_{21j}(x_i - x'_{oj}) + a_{22j}(y_i - y'_{oj}) + a_{23j}(z_i - z'_{oj})}{a_{31j}(x_i - x'_{oj}) + a_{32j}(y_i - y'_{oj}) + a_{33j}(z_i - z'_{oj})}$$

where the index j stands for the variation with the time.

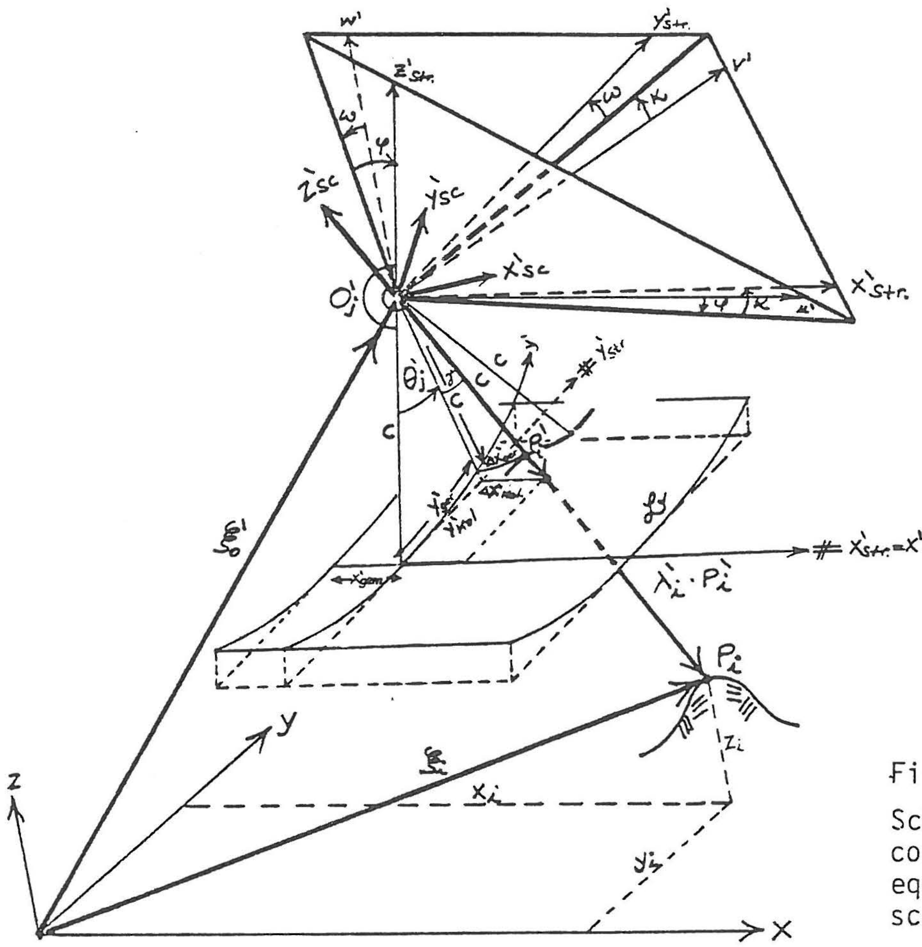

Fig. 1

Scheme to derive collinearity equations for scanner imagery

Subsequently, see figure 1, the needed two dimensional image coordinates are derived from

$$(y') = c \cdot \arctan \left(\frac{c \cdot \tan \theta_{ij}}{c} \right) \tag{2}$$

$$y' = (y') + \sum_{k=1}^{k=n-1\ldots} b_k \cdot {y'}_m^{k} \quad + \ldots b_{\ldots n} {x'}_m^{k'} {y'}_m^{k''} \tag{3}$$

k',k'' see f.i. (16)

$$\Delta x'_c = c \cdot \arctan \left(\frac{\Delta x'}{\sqrt{(y')^2 + c^2}} \right) \tag{4}$$

$$(x') = x'_m + \Delta x'_c \tag{5}$$

$$x' = (x') + \sum_{k=1}^{k=n-1\ldots} a_k \cdot {y'}_m^{k} \quad + \ldots a_{\ldots n} {x'}_m^{k'} {y'}_m^{k''} \tag{6}$$

m = measured c = computed (x') = x' approx. etc.

There are some practical aspects of applying these equations:

3.1 Error elimination

Only for the elimination of gross errors and for deriving the approximate rotation angle (κ) between the terrain coordinate-(x, y, z) and the image-system (x', y') second order polynomials of the form

$$X_{Pol} = A_o + A_1 X'_m + A_2 Y'_P + A_3 {X'_m}^2 + A_4 {Y'_P}^2 + A_5 X'_m Y'_P$$

$$X_{Pol} = B_o + B_1 X'_m + B_2 Y'_P + B_3 {X'_m}^2 + B_4 {Y'_P}^2 + B_5 X'_m Y'_P \tag{7}$$

P = Panoramic corrected Pol = Polynomial approach

are calculated beforehand, where the image coordinates (rows- and columnsvalues) are essential skew-corrected (Landsat only) and panoramic as well as scale corrected of the form

$$y'_P = (y'_m + (\tan \theta - \hat{\theta}) \cdot c) \cdot my' \tag{8}$$

with θ = angle of the instanteneous field of view,

my' = scalefactor for columns relative to the rows.

A representative result for a M^2S image using this polynomial approach in an inverse manner was an obtained accuracy of $\pm$ 7.5 pixels using 167 ground control points.

3.2 Exterior orientation

The collinearity equations are entered with the hypothesis

$$\omega = \phi = 0 \quad ; \quad \kappa = (\kappa)$$

If the accuracy of flight data is too bad or if such data are not available, assumptions for the behavior of the sensor along the flight path are necessary. For this purpose time- respectively equivalent way-functions have been calculated. Here polynomials of the following principle form are used for computing the values of the exterior orientation elements:

$$\omega_j = a_1 + a_2\, x' + a_3\, x'^2 \quad \ldots \quad \text{etc.} \tag{9}$$

However, looking at the differential equations for scanner imagery, which are

$$dx' = c \cdot d\phi + c \cdot \hat{\theta} \cdot d\kappa + (c/h)\, dx_o \quad \text{and}$$

$$dy' = -\,(1 + \hat{\theta}^2) \cdot c \cdot d\omega + (c/h)\, dy_o + (c \cdot \hat{\theta}\,/h) \cdot dz_o \tag{10}$$

the high correlation between $d\phi$ and dx_o is evident. Therefore x'_{oj} was equated with (x'_{oj}).

Consequently the remaining differential equations, which were of 3[rd] order are

$$dx' = c \cdot b_1 + c \cdot b_2 \cdot x' + c \cdot b_3 \cdot x'^2 + c \cdot b_4 \cdot x'^3 + c \cdot \hat{\theta} \cdot c_1$$
$$+ c \cdot \hat{\theta} \cdot c_2 \cdot x' + c \cdot \hat{\theta} \cdot c_3\, x'^2 + c \cdot \hat{\theta} \cdot c_4 \cdot x'^3 \tag{11}$$

$$dy' = -\,c\,(1 + \hat{\theta}^2) \cdot a_1 - c\,(1 + \hat{\theta}^2) \cdot a_2 x' + \ldots + (c/h) e_1$$
$$+ (c/h)\, e_2 \cdot x' + \ldots + (c/h) \cdot \hat{\theta} \cdot f_1 + (c/h) \cdot \hat{\theta} \cdot x' f_2 + \ldots \tag{12}$$

These formulae have been investigated for simulated data, which was a testfield of 600 x 600 m. The flightheight was 300 m and the number of groundcontrolpoints 12, 21 and 30. The result was, that there is a very high correlation (0.96) between ω_j and y_{oj} and also terms depending on x' in a linear manner are not to separate significant from terms depending on x' in higher order. Therefore the exterior orientation data for the rectification of an image of similar size was expressed as

$$\omega_j = a_1 + a_2\, x'_m + \ldots$$

$$\phi_j = b_1 + b_2\, x'_m + \ldots$$

$$\kappa_j = (\kappa) + c_1 + c_2\, x'_m + \ldots$$

$$\begin{pmatrix} x'_{oj} \\ y'_{oj} \end{pmatrix} = \begin{pmatrix} (x'_{oj}) \\ (y'_{oj}) \end{pmatrix} = \begin{pmatrix} x'_{oj_{Null}} \\ y'_{oj_{Null}} \end{pmatrix} + x'_m \cdot \underbrace{h \cdot \frac{\text{resol.}}{1000}}_{\text{const}} \begin{pmatrix} \cos(\kappa) \\ \sin(\kappa) \end{pmatrix} \tag{13}$$

$$z'_{oj} = (z'_o) + f_1 + f_2\, x'_m + \ldots$$

The obtained accuracy expressing the exterior orientation data using first until tenth (!) order polynomials (approach 4 ... 9, see figure 2) oscillate between ± 11.6 pixels and 9.9 pixels, using 126 groundcontrolpoints and 8 ... 44 unknown.

Some elder investigations /7/ deal with spline functions and trivial transition etc. There was not found significant correlation between inflight registrated and computed exterior orientation data. From bundle block adjustment "true" X'_o, Y'_o and Z'_o positions for convential aerial photographs derived. As fortunately for every conventional image the appropriate row value in the simultaneous unconventional image was registrated, fifth order polynomials deliver the sensor platform positions within an accuracy of about $\pm$ 10 m. This knowledge was combined with the following idea of leaving constant platform orientation data for every scanner image row value. The question, if the "correct" statement for expressing the exterior orientation parameters are polynomials, fourier approaches (approach 1 ... 3) Gauss Markov etc. is superfluous because this statements only smooth the physical reality rough.

3.3 Interior orientation

The accuracy increases significant if the formulas for x' and y' contain interior orientation data as unknown additional parameters (approaches 10 ... 12, fig. 2), which can physical give reasons in y' because the platform orientation data change within the scanning of one row or the scanning speed within one line is not constant. This statements are both valid and expressable in the principle formulas (3) and (6). The physical explanation for the interior orientation formula in x' is a distorted scanning-line. In a concrete case a single M^2S image was investigated: The platform positions derived from a conventional aerial photography bundle block adjustment and were interpolated from 16 conventional image positions for the whole scanner image using fifth order polynomials:

$$
\begin{aligned}
X'_{oj} &= (X'_o) + \sum_{k=0}^{k=5} p_k \, X_m^{\prime k} \\
Y'_{oj} &= (Y'_o) + \sum_{k=0}^{k=5} q_k \, X_m^{\prime k} \\
Z'_{oj} &= (Z'_o) + \sum_{k=0}^{k=5} r_k \, X_m^{\prime k}
\end{aligned}
\tag{14}
$$

ω, ϕ, and κ are also expressed using fifth order polynomials

$$
\begin{aligned}
\omega_j &= \sum_{k=0}^{k=5} a_k \, X_m^{\prime k} \\
\phi_j &= \sum_{k=0}^{k=5} b_k \, X_m^{\prime k} \\
\kappa_j &= (K) + \sum_{k=0}^{k=5} c_k \, X_m^{\prime k}
\end{aligned}
\tag{15}
$$

The interior orientation is included by

$$
\begin{aligned}
y' &= (y') + y'_m \cdot u_1 + y_m^{\prime 5} \cdot u_2 + y_m^{\prime 10} \cdot u_3 + x'_m \, y'^{\,8}_m \cdot u_4 \\
x' &= (x') + y'_m \cdot w_1 + y_m^{\prime 5} \cdot w_2 + y_m^{\prime 10} \cdot w_3 + x'_m \, y'^{\,8}_m \cdot w_4
\end{aligned}
\tag{16}
$$

The x'y'-depending terms express physical changing of the interior orientation (changing of ω and ϕ) with the time. Using 126 ground control points an accuracy of $\pm$ 3.7 pixels resulted. Applied to 41 independent check points for the same sample $\pm$ 3.9 pixels were reached, see figure 2 (approach 13). In this test area terrain hights change between 225 m and 625 m, the flight hight was 2300m, the image size 3200 x 800 pixels.

3.4 Stochastic after-treatment

For in the covariance function of the residuals still a signal occured after the interior and the exterior orientation parameters have been calculated, weightened mean interpolation was applied in the form

$$
\begin{aligned}
x'_{interpol} &= x' - \Sigma V_{x'} \, \frac{1}{s'^2} \\
y'_{interpol} &= y' - \Sigma V_{y'} \, \frac{1}{s'^2}
\end{aligned}
\tag{17}
$$

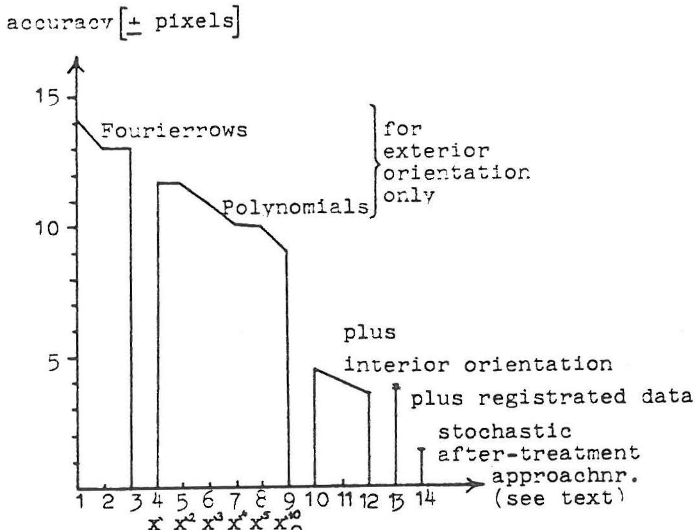

Fig.2 Increasing of M²S-accuracy using different approaches

Fig. 2: Accuracy of M^2S ($\pm$ 1.4 Pixels)

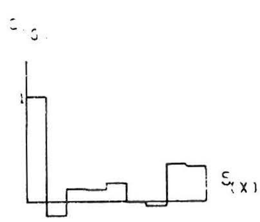

Right:
Fig. 3
Residuals from stochastic after-treatment

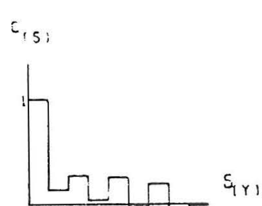

Left:
Fig. 4
Covariance Functions of the residuals from stochastic after-treatment

The accuracy for the 41 checkpoints now became $\pm$ 1.4 pixels, a fantastic result (approach 14, figure 2). The ground control points of course fit frictionless (see figure 3). Figure 4 shows the connected covariance function resulted from the 41 checkpoints.

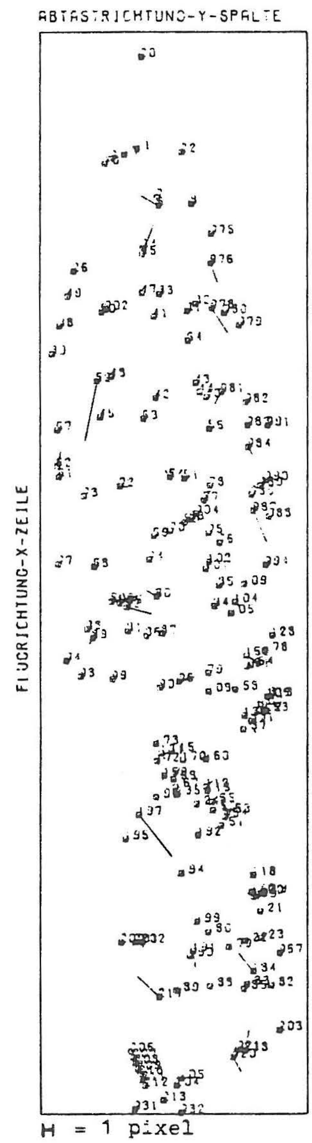

3.5 Practical advices

Looking onto the requir:d high order for x' and y' in the polynomials, rows and column-values have been transfered to the interval + 1 to - 1. Following Düker instead of differential coefficients differences coefficients have been used.

3.6 Bundle block adjustment

The error equations for a bundle block adjustment of overlapping scanner imagery for the first stripe are

$$v_x' = \frac{\partial x'}{\partial \phi} b_1 + \frac{\partial x'}{\partial \phi} x' b_2 + \ldots + \frac{\partial x'}{\partial \kappa} c_1 + \frac{\partial x'}{\partial \kappa} x' c_2 + \ldots + \frac{\partial x'}{\partial x_i} dx_i + \frac{\partial x'}{\partial y_i} dy_i + (\Delta x'_{ger} - 0)$$

$$v_y' = \frac{\partial y'}{\partial \omega} a_1 + \frac{\partial y'}{\partial \omega} x' a_2 + \ldots \frac{\partial y'}{\partial z_0} \cdot f_1 + \frac{\partial y'}{\partial z_0} \cdot x \cdot f_2 + \ldots + \frac{\partial y'}{\partial x_i} dx_i + \frac{\partial y'}{\partial y_i} dy_i + (y'_{ger} - y'_{gem})$$

and for the second stripe (18)

$$v_x'' = \frac{\partial x''}{\partial \phi} b_1' + \frac{\partial x''}{\partial \phi} x'' b'_2 + \ldots + \frac{\partial x''}{\partial \kappa} c'_1 + \frac{\partial x''}{\partial \kappa} x'' c'_2 + \ldots + \frac{\partial x''}{\partial x_i} dx_i + \frac{\partial x''}{\partial y_i} dy_i + (\Delta x''_{ger} - 0)$$

$$v_y'' = \frac{\partial y''}{\partial \omega} a_1' + \frac{\partial y''}{\partial \omega} x'' a'_2 + \ldots + \frac{\partial y''}{\partial z_0} \cdot f_1' + \frac{\partial y''}{\partial z_0} x'' \cdot f_2' + \ldots + \frac{\partial y''}{\partial x_i} dx_i + \frac{\partial y''}{\partial y_i} dy_i + (y''_{ger} - y''_{gem}) \qquad \text{etc.}$$

Practical results showed, it is inopportune to compute terrain hights by this means. A first evaluation of a common calculating of two M^2S stripes show the same results as the single image. In this case, to avoid border inconstancy, the weightened mean statement is expressed as a function of the terrain coordinates:

$$\begin{aligned} x'_{interpol} &= x' - \Sigma V_x' \cdot \frac{1}{s^2} \\ y'_{interpol} &= y' - \Sigma V_y' \cdot \frac{1}{s^2} \end{aligned} \qquad (19)$$

Convergenceproblems did not occur.

4. Application of algorithm onto the pixels using the indirect method

For limiting the core memory space, the rectified image is departed into parallel stripes (à 1719 rows and 150 columns for the sample in figure 7) consisting of rectangular blocks dimensioned in truth with 20 rows and 150 columns instead of 3 rows and 10 columns as it is in principle demonstrated in figure 5. The strong collinearity equations are only applied onto the 4 with x, y and z pretexted centers of the block edges (anchor-points = cross marks in figure 5), where the resulted 4 image coordinates (row - (= record-) and column values) address the needed core memory, which are actual 110 x 210 greyvalues instead of 4 x 7 greyvalues as drawn in figure 5, following Bernstein et all /8/. The image coordinates (corememory positions) of the other out-pixel-centers within the block are interpolated using hyperbolic transformation. To conservate image information and contrast, minimum scale changes and nearest neighbour greyvalue interpolation are realized, as well as compared with Kraus /9/, the nature of the greyvalues after the rectification process is still digital. The D.T.M. data were gathered from topographic maps (scale 1 : 5000), using a gridinterval of 200 m, and stored on a magnetic disc. The D.T.M. is not yet used for automatic isoline overlay generating but for compensation of distortions caused by differences in the terrain hights.

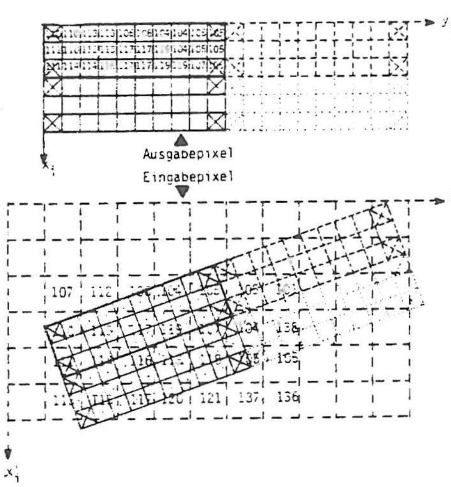

Fig. 5: Scheme of "continuous memoring" to complete the orthophoto

To minimize the effective disc readingtime in many cases it seems to be expedient to rotate the D.T.M. digital in forehand. According to figure 6, the x_B and y_B coordinates of the rotated D.T.M. are original x and y:

$$\begin{pmatrix} x \\ y \end{pmatrix} = \begin{pmatrix} x_{0B} \\ y_{0B} \end{pmatrix} - \begin{pmatrix} \cos\beta & -\sin\beta \\ \sin\beta & \cos\beta \end{pmatrix} \begin{pmatrix} x_B \\ y_B \end{pmatrix} \qquad (20)$$

To compute the terrain hights H_i for the gridpoints of the rotated D.T.M. as well as the terrain hights of the anchor points, occasionally hyperbolic interpolation within the four D.T.M. edges was applied:

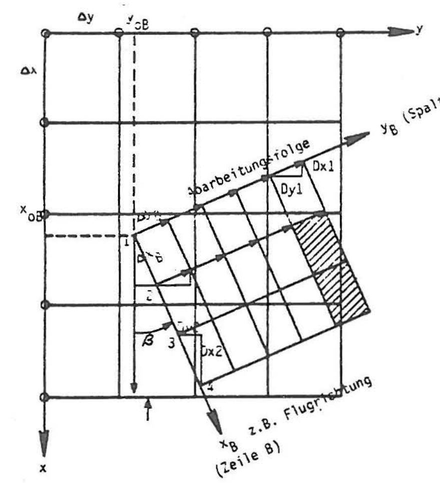

Fig. 6: Digital D.T.M. Rotation

$$H_i = a_I + a_{II}\, x_i + a_{III}\, y_i + a_{IV}\, x_i y_i \tag{21}$$

Following Rüdenauer /1/ the type of interpolation method is not as important as the D.T.M. gridinterval-length. Using the indirect rectification method, the strong entry points of the collinearity equations, which are the measured image coordinates, were left, because for the output pixels are only known the map coordinates and interpolated terrain hights, but not the corresponding, from the dataanalysis obligate required measured image coordinates, which shows, scannerimages are not "strongly" to rectify. To solve this problems, equations (22)

$$\begin{aligned} x'_{rec\ I\ldots} &= (x')_{I\ldots} + \frac{\partial (x')_{I\ldots}}{\partial \Delta x'_{cI\ldots}} \cdot \Delta x'_{CI\ldots} \\ y'_{recI\ldots} &= (y')_{I\ldots} + \frac{\partial (y')_{I\ldots}}{\partial (y')_{CI\ldots}} \cdot ((y')_{CI\ldots} - (y')_{I\ldots}) \end{aligned} \tag{22}$$

rec = rectified I... = number of iteration step

normally were iterated 7 times, until there was no significant change in the x'_{rec} as well as in the y'_{rec}. Provable the result is independent of the very first approximation values $(x')_I$ and $(y')_I$ for which f.i. can be used the results of a polynomial approach for x' and y', in the 2nd iter. $(x')_I$, $(y')_I$ are x'_{rec}, y'_{rec} etc.. The divergence between x' and y' of formula (16) and x'_{rec}, y'_{rec} of formula (22) is about the size of the residuals.

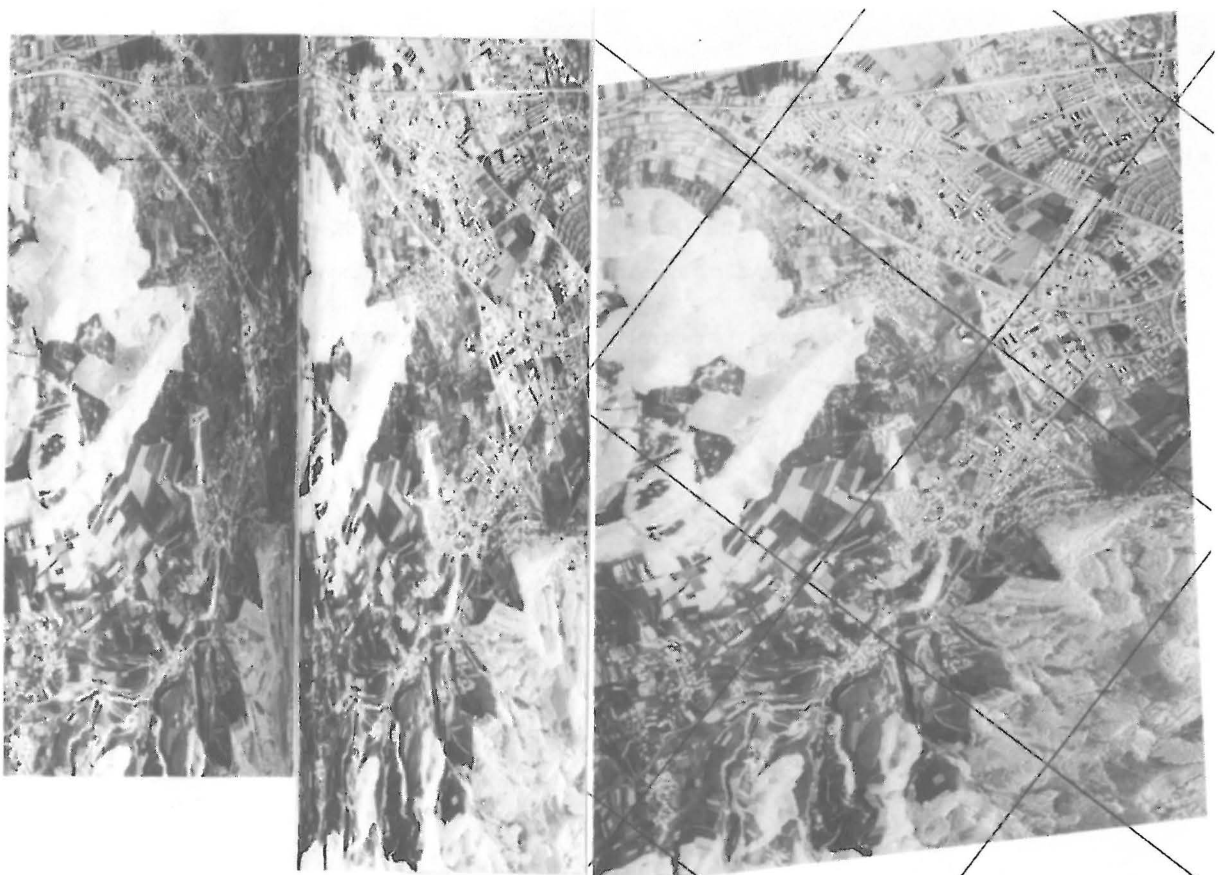

Fig. 7: Overlapping M^2S images and rectified product (Freiburg, Black Forest)

For the "application equations" (22) and not the "analysis equations" (16) are in practise useable for the pixelwise rectification, in truth in (17)

$V_x' = -x'_{meas} + x'_{rec}$ and $V_y' = -y'_{meas} + y'_{rec}$ as well as x' and y' in (17) become x'_{rec} and y'_{rec}, where for weightened mean interpolation x'_{meas} and y'_{meas} fit precisely in the ground control points, see figure 3. In figure 7 is demonstrated a sample for two overlapping M^2S stripes consisting of about 1700 rows and 600 columns. The geometric processed image in original has the scale 1 : 50 000, is digital overlayed with a 2 x 2 km grid, flypath oriented and processed on an optronics P 1700 device.
The program already allows the rectification of larger image blocks (sceneries) of one cast, th. i. without transitions belonging to geometry and radiometry.

5. Acknowledgements

The author is grateful to ISP 80 Congress-Dir. Prof. Dr. Konecny for the opportunity to investigate this topic and for the helpful suggestions, to the German Research Society (DFG) and to the D.F.V.L.R., which generously sponsored this work. Calculations have been carried out on the C.D.C. Cyber 7 6 - 12 Computer of the Regional Computing Center of Lower Saxony.

6. References:

/1/ Rüdenauer, H.: Zur photogrammetrischen Datenerfassung und ihrer digitalen Verarbeitung unter Berücksichtigung straßenbaulicher Forderungen. Diss., Hannover 1980

/2/ Jacobsen, K : Vorschläge zur Konzeption und zur Bearbeitung von Bündelblockausgleichungen. Diss., Hannover 1980

/3/ Baker, J.R. and Mikhail, E.M. : Geometric analysis and restitution of multispectral scanner arrays. LARS Information Note 052875, Purdue-University, West Lafayette, Indiana, 1975

/4/ Anuta, P. : Digital Registration of Topographic Data and Satellite MSS Data for Augmented Spectral Analysis. Proc. of the ASP 42nd animal meeting, 1976, S. 180 - 187

/5/ Bernstein, R. and Ferneyhough, D. G.: Digital Image Processing. Phm. Eng. XLI (1975) S. 1465 - 1476.

/6/ Konecny, G. : Mathematische Modelle und Verfahren zur geometrischen Auswertung von Zeilenabtaster-Aufnahmen. BuL 5/1976, S. 188 - 197

/7/ Schuhr, W. : Digitale Entzerrung multispektraler Bilder. BuL 5/1976, S. 202 - 208

/8/ Bernstein, R., Depew, R. and Murphrey, S.: Digital Processing of Conical Scanner Data. Phm. Eng. Vol. 43 (1977), S. 155 - 167

/9/ Kraus, K. : Applications of a digitally controlled orthophoto instrument. Presented Paper: Comm. IV, XIII International Congress for Photogrammetry, Helsinki 1976